Design of a Switching Power Supply

Jake Roller

14 October 2022

Contents

1 Overview

A DC-DC switching power supply is both a useful and challenging design opportunity, given the right guiding specifications. Switching power supplies are versatile and essential systems that are able to be tailored for powering rocket avionics (flight computers) and UAV peripherals.

Currently, WPI's High Power Rocketry Club (HPRC) builds its avionics boards with linear regulators which, while cheap and easy to implement, are not ideal for high-power applications due to their significant inefficiencies. Implementing an efficient switching regulator allows for longer battery life and more versatile input selection. This project served as a valuable learning experience including design, analysis, fabrication, and test of a switching power supply module, an introduction to modern power electronics, as well as an introduction to product design and rapid prototyping of an electronic system.

1.1 Project Scope

The scope of this project was to create a switching power supply, aiming to be a "Battery Eliminator Circuit" (BEC) which allows for a wide range of batteries to be used to power lower-voltage electronic systems. More specifically, the project included an initial study of feasibility, followed by high-level design and requirements definition. This was followed by both circuit- and component-level calculations, allowing for component selection and schematic capture. Using the schematic, a printed circuit board (PCB) was designed using special considerations for high-frequency and high-current switching applications, manufactured, and tested to determine the actual performance of the system.

2 Specifications

Considering the use-case of the switching power supply module (providing battery power to avionics systems), high level specifications were fairly simple to define. Below, in Table 2.1 are the high-level requirements which are derived in the following subsections.

Table 2.1: High-Level Requirements

Requirement	Variable	Value
Minimum Input Voltage	$V_{in_{min}}$	3.7 V
Maximum Input Voltage	$V_{in_{max}}$	25.2 V
Output Voltage	V_{out}	3.3 V
Maximum Load Current	$I_{out_{max}}$	2 A

2.1 Input Voltage Range

The input voltage range was set based on the voltage range of common Lithium Polymer (LiPo) and Lithium Ion (Li-ion) batteries. The voltage of a single-cell LiPo battery ranges from $3.7 - 4.2$ V when charged properly. This is a good starting point, however batteries are often be connected in series and parallel to increase voltage or capacity, as often done by battery manufacturers. The number of cells in parallel determines the current and storage capacity of the battery which is not a concern for defining the input voltage; only the total number of cells in series is important in this regard. LiPo batteries are commonly available in configurations anywhere from 1s to 6s, where 's' denotes series. This allows us to determine the minimum and maximum input voltages required for the switching power supply.

The minimum input voltage requirement comes from the 1s battery, as it has the fewest number of cells in series and thus the lowest voltage when at low charge.

$$V_{in_{min}} = 3.7\,\text{V} \cdot 1 = 3.7\,\text{V} \tag{2.1}$$

The maximum input voltage requirement can be derived using the largest battery size desired: 6s, as it has the most cells in series and thus the highest voltage at full charge.

$$V_{in_{max}} = 4.2\,\text{V} \cdot 6 = 25.2\,\text{V} \tag{2.2}$$

2.2 Output Voltage

The required output voltage was set based on the intended use of the power supply. Microcontrollers commonly require an input 3.3 V, and most microcontrollers that are considered for future use with HPRC's avionics will run on 3.3 V. Thus, the output voltage of the switching power supply is required to be 3.3 V to directly power the microcontroller, sensors, and supporting components.

2.3 Maximum Load Current

The maximum load current is a crucial defining requirement for any switching power supply, as it determines the capability of the supply as well as the current handling requirements for all switching components. Previous avionics systems for HPRC have required anywhere from 100 to 750 mA of current, however that number is expected to grow significantly as more power-hungry components such as radios and GPS modules are added. A load current requirement of 2 A was determined by current estimates for various future avionics designs which are outside the scope of this project.

3 Circuit Design

Most step-down (buck) switching power supplies have a very similar basic schematic layout as pictured in Figure 3.1. In the schematic input voltage source is listed as V_s, although it is defined as V_{in} in this project for clarity. The resistor in the schematic symbolizes a generalized ohmic load, with V_o being the output voltage which is defined as V_{out} in this project. Similarly, the current going through the load resistor is labeled i_R in the schematic but is defined as I_{out} in this project.

The schematic in Figure 3.1 consists of six main elements: the input voltage source, a switching element, an inductor, a diode, an output capacitor, and a load resistor. The switching element is simplified and drawn as an ideal switch, however in reality this switching element is generally implemented as a MOSFET. Despite some simplifications, this general schematic serves as a sound foundation for sizing components.
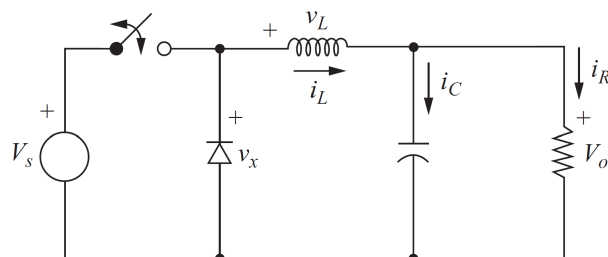

Figure 3.1: Generic buck DC-DC converter. [2]

4 Component Selection

From the basic circuit design discussed in Section 3, there exists a list of essential components needed to create the switching power supply. While Figure 3.1 breaks out the switching element and diode as discrete components, these components are often integrated into one integrated circuit (IC) called a switching controller. This leaves a list of only three major components in the switching circuit: switching controller, inductor, and output capacitor. This list is not extensive however, and most switching controllers require supporting components to function properly.

4.1 Switching Controller

As the heart of the switching power supply, the selection of the switching controller IC is crucial. Performing a simple search on DigiKey, an online electronics distributor, returns an astounding 2,330 step-down switching controllers that are in stock and recommended for new designs (active parts). This number is somewhat deceiving however, as when we add filters for the ICs to meet or exceed the requirements discussed in Section 2, the number of results is brought down to 466.

To further narrow the search, a desired range was decided for switching frequency of $400 - 500$ kHz. This is a standard range, chosen as it provides a good balance between providing a high switching frequency to reduce output ripple frequency and inductor size, while not interfering with higher-frequency RF electronics used to transmit rocket telemetry which operate in bands around 915 MHz. Additionally, this frequency range is well above the human hearing limit of 20 kHz, meaning the switching operations should be inaudible, and the device should produce no audible "coil whine".

From this final search, the Diodes Incorporated AP63356 switching controller stood out as the clear choice with a switching frequency of 450 kHz, a higher-than-required 3.5 A maximum output current which provides a safety factor of 1.75 above the required 2 A output current. The input voltage range of this switching controller is $3.8 - 32$ V which easily satisfies the $V_{in_{max}}$ requirement, however fails to satisfy the $V_{in_{min}}$ requirement. This was deemed acceptable, however, as discharging a LiPo under 3.7 V can cause damage to the cells meaning the minimum voltage of the switching controller acts as a rudimentary over-discharge protection for the connected battery.

4.2 Inductor

Selecting the inductor for the switching power supply relies first on knowing the inductance required. Determined in Section 5.4, $L = 4.7\,\mu\text{H}$. With this value and the maximum inductor switching current of $I_{sw_{max}} \approx 3\,\text{A}$ calculated in Section 5.3, a search was conducted for inductors to meet these requirements. From this search, the SRP4030FA-4R7M inductor from Bourns Inc. was selected. This inductor has a footprint of 0.161" × 0.161" and is 0.118" tall which is significantly smaller than most other inductors in its class. It has a maximum current rating of 5.1 A which is well above the requirement for inductor switching current, and has a self resonant frequency of $27\,\text{MHz}$ which is far from the switching frequency of the controller $f_{sw} = 450\,\text{kHz}$.

4.3 Output Capacitor

The output filtering capacitor for the switching power supply was chosen from the switching controller's datasheet. For the 3.3 V output configuration, a minimum output capacitance of $22\,\mu\text{F}$ is recommended. To improve filtering characteristics, two $22\,\mu\text{F}$ capacitors in parallel were selected as the output capacitor. As the output capacitor only needs to handle the 3.3 V output from the power

supply, a 6.3 V 0805 capacitor from Samsung Electro-Mechanics was chosen. The 0805 footprint provides ample space for soldering and touch-up and reduces price at larger capacitances.

4.4 Feedback Resistors

The selected switching controller requires a voltage divider to feed a known fraction of the output voltage back into the internal control loop. This is accomplished by constructing a voltage divider between the output voltage and ground. As with most integrated switching controllers, the AP63356 actively controls its feedback voltage to 0.8 V. From the calculations done in Section 5.5, $R_1 = 93.75\,\text{k}\Omega$ and $R_2 = 30\,\text{k}\Omega$. The value of R_1 was not determined to be an E12 value and thus sourcing a resistor of exactly that resistance would be difficult and costly, therefore a modified resistance of $R_1 = 91\,\text{k}\Omega$ was chosen as the closest commonly available resistance value. Using Equation 5.6 and the actual voltage divider resistances, the output voltage will be $V_{out} = 3.23\,\text{V}$ which is within an acceptable range for a microcontroller's supply. With tolerance on the resistors, this was a possible output voltage even with the initially calculated ideal resistance values.

For the feedback voltage divider, 0402 package resistors were chosen due to their small size and abundance allowing for a smaller overall system footprint and cost-effective sourcing. The resistors were sourced from Stackpole Electronics Inc, have a tolerance of $\pm 1\%$, and are capable of dissipating 1/16 W.

4.5 Feedback Decoupling Capacitor

The typical application circuit for the chosen switching controller recommends the addition of a small decoupling capacitor between the output and the feedback nodes. Per the datasheet, the value of this capacitor was chosen as $C_4 = 33\,\text{pF}$. This capacitor was sourced from Kyocera AVX in an 0402 footprint to match size of the feedback resistors selected in Section 4.4.

4.6 Bootstrap Capacitor

The AP63356 switching controller requires a bootstrap capacitor that feeds from the switching pin of the IC. This capacitor is set by the manufacturer to $C_3 = 100\,\text{nF}$. An 0603 footprint capacitor from Samsung Electro-Mechanics was chosen for the bootstrap capacitor due to its ease of integration and low-cost delete.

4.7 Input Capacitor

The input capacitor serves as a decoupling capacitor across the power supply's input, reducing noise in the high-voltage supply. As per the switching controller datasheet recommendations, its capacitance was set to $C_1 = 10\,\mu\text{F}$ to adequately decouple the input supply. Despite its large size, a 1206 footprint capacitor from Samsung Electro-Mechanics was chosen for the input decoupling capacitor due to its large capacitance and low cost.

5 Analysis

5.1 Duty Cycle

Equation 5.1 can be used to determine the duty cycle of the switching power supply [2]. Using values from the requirements and an efficiency $\eta = 0.8$ from the switching controller's datasheet,

the duty cycle can be found as $D = 0.1375$.

$$D = \frac{V_{out}}{V_{in_{max}} \, \eta} \tag{5.1}$$

5.2 Inductor Ripple Current

Ripple current through the inductor is an important characteristics of switching power supplies, as it determines the noise generated by the system. Lower values of inductor ripple current lead to lower noise, both in the output current and in the EMI emission from the power supply. Equation 5.2 details how to calculate the inductor ripple current for a given input voltage. This is used later, in Section 5.4 to determine the required inductor value.

$$\Delta I_L = \frac{D \, (V_{in} - V_{out})}{f_{sw} \, L_{avg}} \tag{5.2}$$

5.3 Switching Current

Equation 5.3 governs the peak switching current through the inductor. Using values calculated previously, the peak switching current can be found as $I_{sw_{max}} \approx 3\,\mathrm{A}$.

$$I_{sw_{max}} = I_{out_{max}} + \frac{\Delta I_L}{2} \tag{5.3}$$

To verify that the maximum current going through the switching controller is within its capabilities, we can use Equation 5.4 and $I_{LIM_{min}} = 4.2\,\mathrm{A}$ from the switching controller's datasheet to arrive at a value of $I_{IC_{max}} \approx 3.2\,\mathrm{A}$. The absolute maximum current of the switching controller is $5\,\mathrm{A}$, which the maximum current is well below.

$$I_{IC_{max}} = I_{LIM_{min}} - \frac{\Delta I_L}{2} \tag{5.4}$$

5.4 Inductance

To determine the minimum inductance required, we start with Equation 5.5. Using values discussed previously and an estimate of 20% ripple current, the minimum inductance required is found to be $L_{min} = 10.878\,\mu\mathrm{H}$.

$$L_{min} = \frac{V_{out} \, (V_{in_{max}} - V_{out})}{\Delta I_L \cdot f_{sw} \cdot V_{in_{max}}} \tag{5.5}$$

To refine the inductance value, we can look to minimize the inductor ripple current as well as the disparity in inductor ripple current over the range of input voltages. Using Equation 5.2, we can plot the inductor ripple current over the input voltage range at a range of inductances. As seen in Figure 5.1, a higher inductance results in a lower ΔI_L, however this effect is reduced as inductor values get larger. Although a higher inductance is desirable, it increases cost and physical size of the inductor. With this and the E12 series of common values in mind, an inductor value of $L = 4.7\,\mu\mathrm{H}$ was selected. Comparing the selected inductance with the minimum inductance value from Equation 5.5 of $L_{min} \approx 11\,\mu\mathrm{H}$, we can see that our selection falAlthough initially, this seems to indicate an error in the calculations, re-calculating the minimum inductance using Equation 5.5 with an updated inductor ripple current of $\Delta I_L \approx 1.5\,\mathrm{mA}$, the minimum inductance is now $L_{min} = 4.351\,\mu\mathrm{H}$. Additionally, the manufacturer's datasheet for the switching controller suggest an inductance range of 4 - 6 $\mu\mathrm{H}$ for an output of 3.3 V which confirms the $4.7\,\mu\mathrm{H}$ choice.
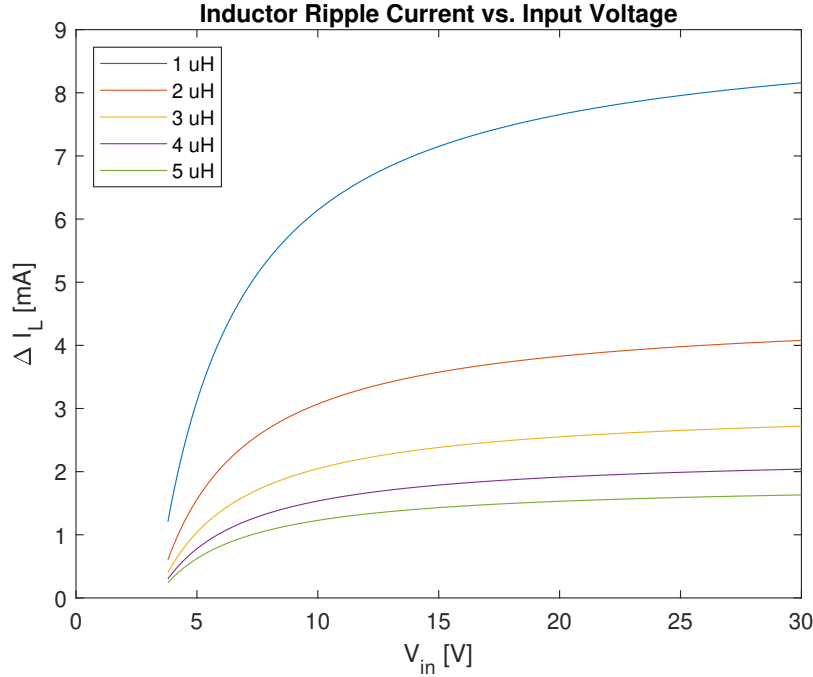
Figure 5.1: Inductor ripple current plotted against input voltage for a range of inductances.

5.5 Feedback Voltage Divider

Equation 5.6 can be used to determine the resistor values needed to meet the 0.8 V feedback voltage requirement of the switching controller. To keep the noise to a minimum while also reducing current consumption of the resistor divider network, the kilo-ohm range was selected. Sleeting an arbitrary value of $R_2 = 30\,\text{k}\Omega$ and the output voltage of $V_{out} = 3.3\,\text{V}$, $R_1 = 93.75\,\text{k}\Omega$.

$$R_1 = R_2 \cdot \left(\frac{V_{out}}{0.8\,\text{V}} - 1 \right) \tag{5.6}$$

5.6 Thermals

Due to the high-current requirements discussed in Section 2, thermal dissipation was a major point of concern during the design of the switching power supply. The switching controller datasheet provided confidence in the form of indicating minimal temperature rise with increasing current, leaving PCB design and mounting the two remaining considerations for thermal control. As discussed in Section 6.2, large polygons of copper were chosen to increase thermal capacity over the traditional trace method of routing circuit boards.

Figure 5.2 shows the results of a custom calculator to model the temperature rise of copper traces at 2 A as plotted against a varying trace width. With a 24 mil trace width, the temperature rise would be approximately 20 deg C which is an acceptable temperature rise. As copper polygons with widths much greater than 24 mils were used, the thermal dissipation of the PCB copper was deemed sufficient.
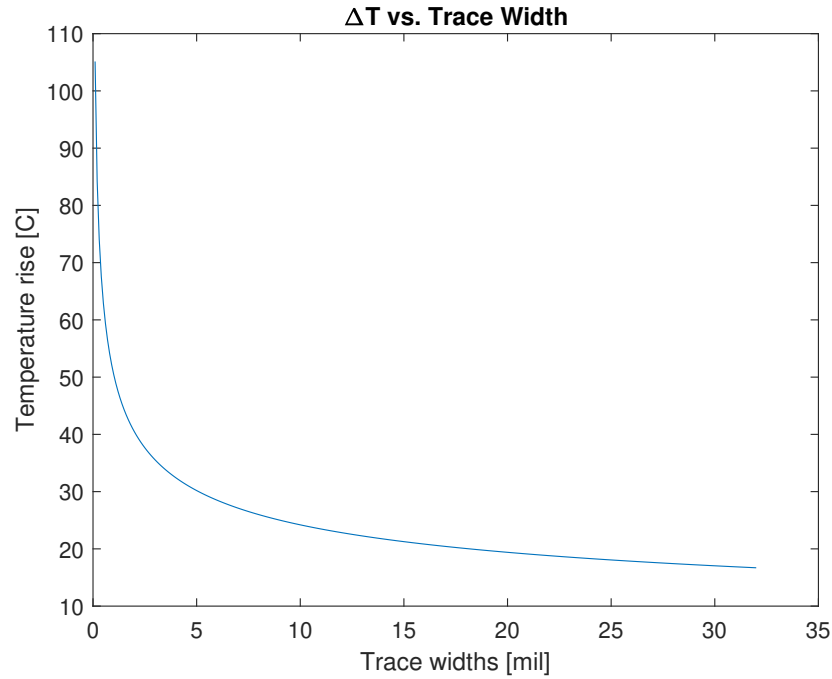
Figure 5.2: PCB Trace Temperature Rise vs. Trace Width.

5.7 Simulations

Simulations of the switching power supply were conducted in LTspice using component properties detailed in Section 4. Simulations indicated proper operation of the circuit across all required input voltages, providing a steady 3.3 V output with minimal ringing. No saturation or other high-current effects were observed for larger loads.
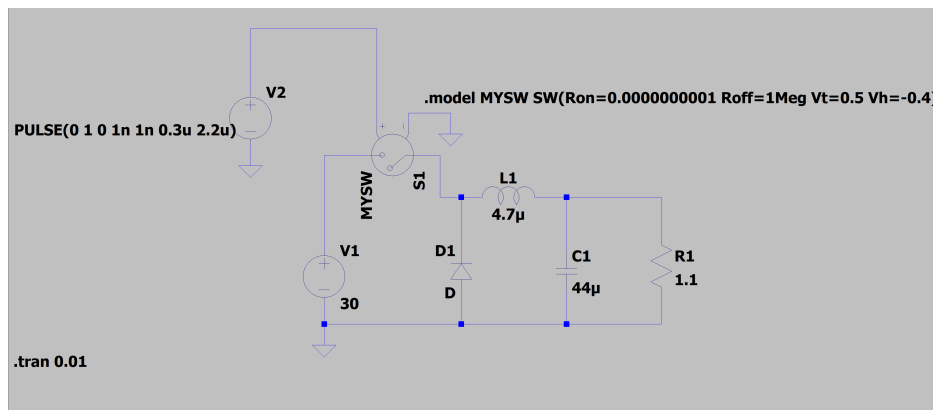

Figure 5.3: Switching Circuit as Simulated in LTspice.

6 Design

6.1 Schematic Capture

Schematic capture for this project was completed in Autodesk EAGLE. A custom library part (schematic symbol and PCB footprint) was created for the AP63356 switching controller. From

this, the supporting components and circuitry were laid out in a similar fashion to most DC-DC buck converters, paying close attention to the datasheet's recommended application circuit as well. The values for the passive components are as discussed in Section 4. Two components that were not discussed previously are J1 and J2. These are pin-header connectors that serve as the power supply's connection to the high-voltage input and 3.3 V output rails. These power rails, and a common ground, are sourced from these connectors, with their symbols being used in the rest of the schematic to signify an electrical connection. C2, the output decoupling capacitor discussed in Section 4.3 was split up into two parallel capacitors: C2.1 and C2.2 to provided further output decoupling capacity. With the final schematic pictured in Figure 6.1, the PCB layout and routing could be conducted, as detailed in Section 6.2.
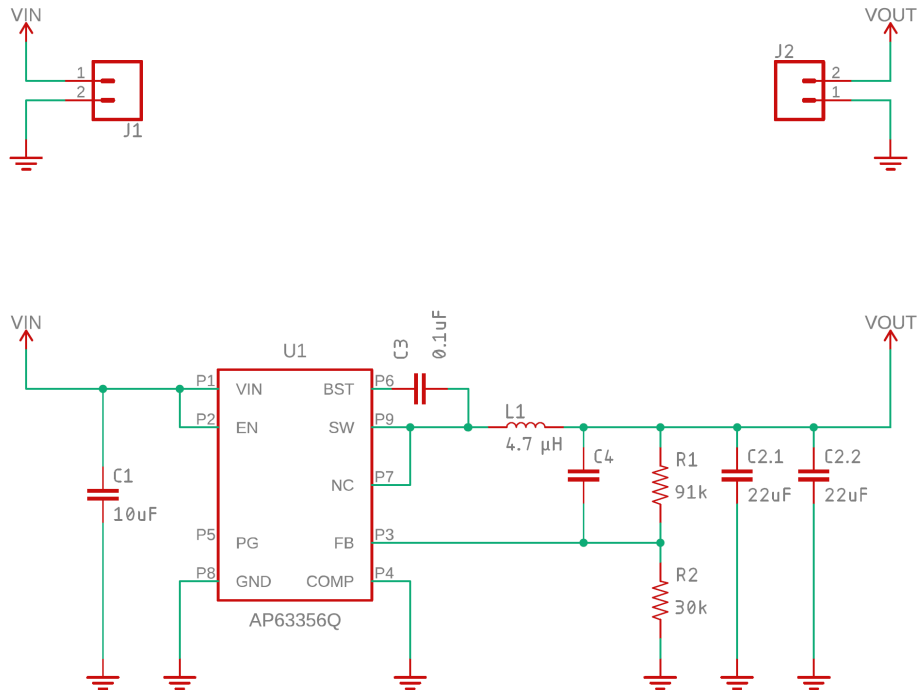

Figure 6.1: Switching Power Supply Schematic.

6.2 PCB Layout

As with the schematic capture, the PCB layout and routing for this project were completed in Autodesk EAGLE. With the schematic complete, EAGLE generated a board file with all of the components with their footprints in no particular meaningful order. The position of these footprints in relation to each other is a key factor in determining the success of any switching power supply design, with important considerations for current handling, EMI, and more. The datasheet for the AP63356 switching controller provides a baseline layout as seen in Figure 6.2 and a fairly extensive list of layout considerations to aid in the PCB design process.
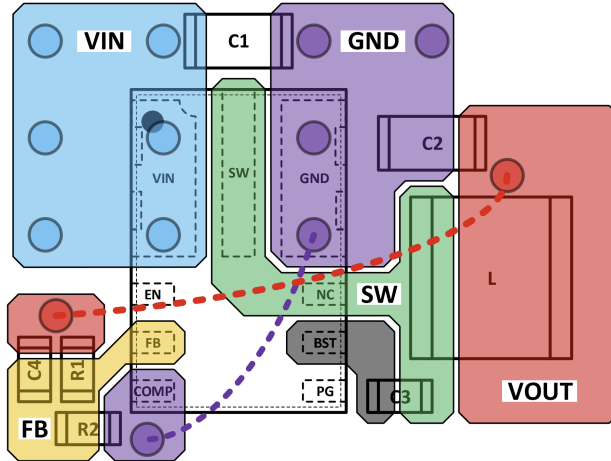
Figure 6.2: Baseline layout from AP63356 datasheet. [1]

Although the recommended layout provides a solid baseline to work off of, it has several factors that make it non-ideal for this design. The main factor that detracts from this layout is its size. Additionally, the components in the recommended layout are laid out in a way that does not consider hand assembly. Although most commercial boards are assembled by CNC pick-and-place machines, prototypes such as this board are often assembled and soldered by hand which leads to a considerable lack of precision and repeatability.

In EAGLE, a new layout was created, void of a board outline, to determine the minimum possible board size using similar considerations as used in the datasheet. As seen in Figure 6.3, the layout is similar to that in Figure 6.2, with a few major changes. The input and output pin-header connectors were placed on the left- and right-hand sides of the board, respectively to match the layout of certain COTS BEC modules. This input-output configuration lends itself well to integration on other circuit boards, and makes layout of those boards significantly less complex.

Additionally, all of the components chosen in Section 4 are larger than those in the baseline layout. If Figure 6.2 is drawn to scale, the components used are extremely small with C1 being at most an 0402 component. This disproportionate scaling leads to the need for significant layout changes, for example the placement of C3 and L1 with respect to each other and the switching IC. The layout in Figure 6.3 uses all of the final component sizes laid out in a way that is conducive to hand soldering, leaving space for a soldering iron tip in case touch-up is needed. The main change in layout aside from component size is the location and quantity of the output decoupling capacitors. As mentioned in Section 4, the output capacitor C2 was split into two and is placed closest to the output pin headers. Although it looks visually different than the placement in baseline layout, the new output capacitor placement keeps the same priority of proximity to the output pads.
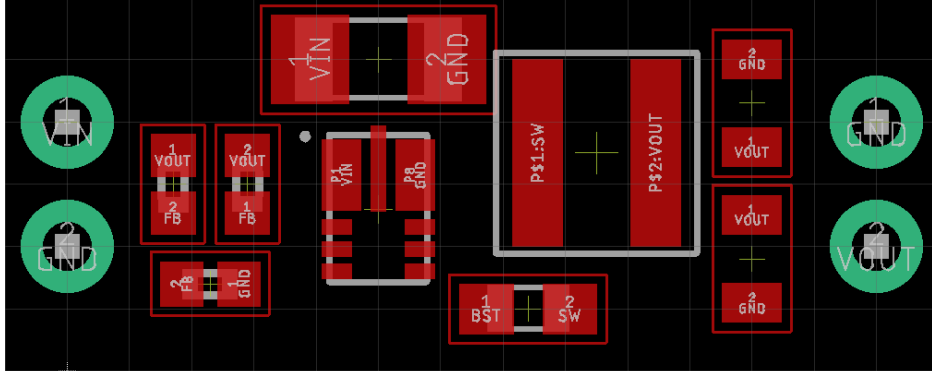
Figure 6.3: Preliminary Unrouted Layout in EAGLE.

Using the finalized component layout, the board dimensions were set with the intention of keeping the system as small as possible. To achieve this, and to aid in future integration efforts, the input-output pin headers were placed with their centers on the edge of the board outline turning them into castellated holes. This allows for both through hole mounting when desired and surface mount assembly when the absolute lowest profile is desired. With this constraint set, the length was easily determined to be 0.65". Although less constrained, the width of the board could be set using a reasonable distance offset from the outermost components, leaving the width to be 0.30".

Typically electrical connections on PCBs are made using traces, which are lines of copper drawn with a constant thickness. This is a good method for routing low-speed and low-current signals, however it leads to significant heat buildup with higher currents while each trace acts as a small antenna at high-frequencies. Since this switching power supply is both a high-current and high-frequency device traditional trace-routing PCB design methods were not suitable. Instead, for switching power supplies, it is best practice to use polygons (or 'pours') of copper to complete electrical connections as seen in Figure 6.2. These polygon connections are not only favorable for current and RF reasons, but the large polygons of copper also act as a heat sink to aid in thermal dissipation for the switching IC itself along with the copper temperature rise discussed in Section 5.6.

Pictured in Figure 6.4, the final layout of the board includes polygons for almost every electrical connection, except for the feedback tap-off from the V_{out} polygon which is routed as a trace on the underside of the board as seen in Figure 6.5. The rest of the underside of the board is left as a solid polygon of copper connected to GND through vias and the castellated edge connectors.
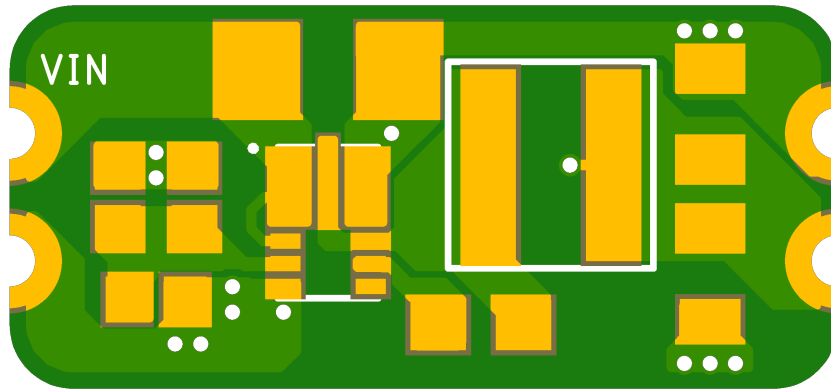
Figure 6.4: Final PCB Layout (Top Layer).

Figure 6.5: Final PCB Layout (Bottom Layer).

7 Assembly

With the layout completed in Section 6.2, the switching power supply board was ready for manufacture, assembly, and test. Due to the small size and urgency of the design, OSH Park, was selected as the preferred manufacturer for the PCBs themselves, while DigiKey was selected for component distribution.

The manufacturer, OSH Park noted that an error occurred during the manufacturing of the boards. Two of the nine boards ordered were salvageable and delivered, however only after great delay. Before assembly, the board needed to be mechanically cleaned which resulted in the empty board shown in Figure 7.1.
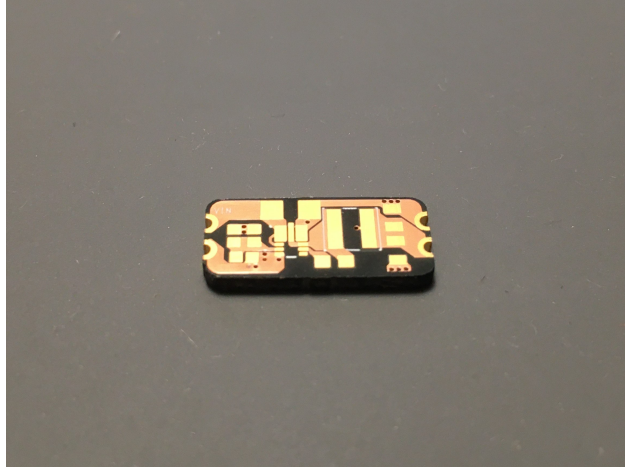
Figure 7.1: Cleaned PCB.

Using a stencil manufactured by OSH Stencils, solder paste was applied through the apertures to all of the pads as pictured in Figure 7.2. With the solder paste applied, components were placed on the board, each in their respective locations according to the board layout. Finally, the solder was reflowed using a hot air workstation and all components were soldered into place.
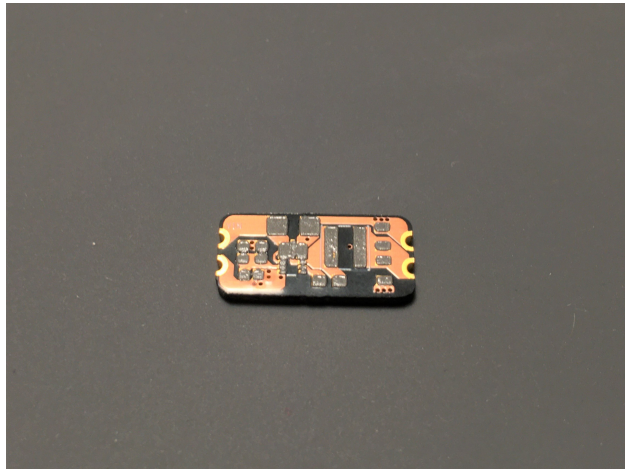

Figure 7.2: PCB with Solder Paste Applied.

The final, assembled board can be seen in Figure 7.3. The PCB significant touch-up due to the imprecision introduced with hand assembly and hot-air reflow. Upon visual inspection, there were multiple solder shorts between pins on the switching controller IC. Using a microscope as seen in Figure 7.4, the shorts were identified and removed using a fine-point soldering iron.
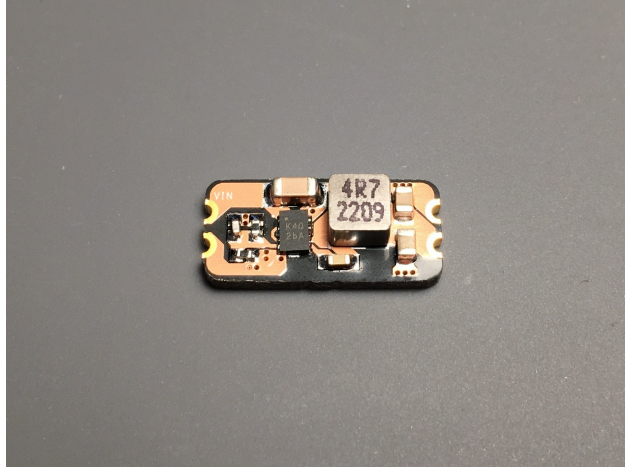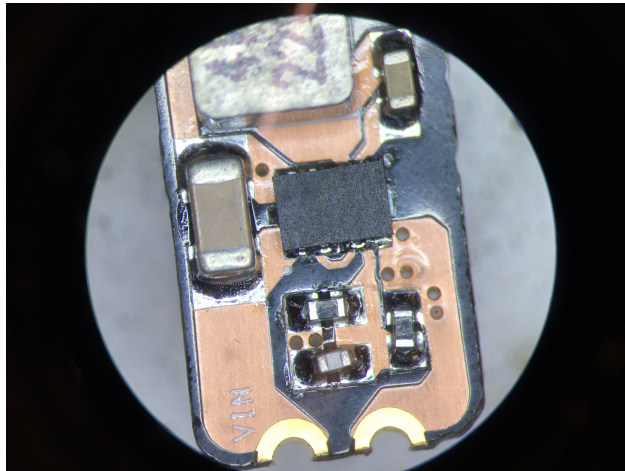
Figure 7.3: Assembled Switching Power Supply PCB.

Figure 7.4: PCB Viewed with Microscope Showing Shorts.

8 Test

After the board had been fully assembled and was free of shorts, the switching power supply was ready for test. Due to the delay in fabricating the boards at OSH Park, there was not much time left for extensive testing. Instead, abbreviated tests were conducted simply with a DC power supply and a multimeter.

When the input pins were connected to the output of the DC power supply set to 5 V, the output of the buck converted was measured to be only 0.8 V between V_{out} and GND. As 5 V is at the lower end of the range of designed inputs for the power supply, the output voltage of the DC power supply was increased to 8.4 V to simulate a 2s LiPo battery, and then 12 V for an even higher voltage. At all of these input voltages, the step down converter consistently regulated the output voltage of 0.8 V.

The initial tests with the DC power supply were conducted in the no-load condition, with no load placed across the output of the switching power supply. Although some switching power supplies can be susceptible to noise and adverse operations under the no-load condition, the AP63356 switching controller chosen for this project claims to operate nominally under no load. However, to rule out

the possibility of the improper operation being caused by the no-load condition, a 500 Ω was placed across the output to simulate a load. The same input voltage tests were conducted with the artificial load, and the system operated the same, regulating any input voltage to 0.8 V.

Due to the time constraint, one final test was conducted in an attempt to diagnose the improper operation of the system. Since the switching controller regulates the voltage with an internal control loop which takes the 0.8 V feedback voltage as its input, the feedback voltage divider discussed in Section 5.5 was inspected. Measuring resistance, both resistors R_1 and R_2 were measured to be within the 1% tolerance claimed by the manufacturer, ruling out the possibility of an improper feedback network.

9 Future Work

As the testing regime for this project was abbreviated due to lack of time, further tests are required to diagnose the root cause of the malfunction. The first test that should be conducted in the future is to use an oscilloscope to observe the switching behavior of the system. By attaching a probe to the switching pad of the bootstrap capacitor, the switching output of the controller can be observed to determine if the controller is functioning properly.

The AP63356 switching controller used in this project also contains a PG, or power-good, pin that is pulled high when the controller senses it is in nominal operation. Although this pin was left unconnected in the initial revision, a future revision of the PCB could break out this signal to a test point for testing.

Using an oscilloscope to measure the output of the switching power supply would allow for further inspection of the output and might provide more insight into the operation. The voltage measurements referenced in Section 8 were conducted using a simple multimeter measuring DC voltage. Using an oscilloscope would allow for observation of any AC or transient effects present on the output which could indicate specific issues.

There are more measurements that can be conducted to further diagnose the operation of the switching power supply. These include checking for a proper soft-start, ensuring proper duty cycle, and improper oscillation [3].

Future improvements to the system aside from restoring proper operation include adding a second output rail for 5 V devices such as servos and other actuators, as well as increasing the copper thickness to 2oz to ensure better thermal dissipation.

References

[1] AP63356Q/AP63357Q datasheet. 2020.

[2] D. Hart. *Power Electronics*. WCB/McGraw-Hill, 2010.

[3] Pradeep Shenoy. Common mistakes in dc/dc converters and how to fix them. *2018 Texas Instruments Power Supply Design Seminar*, 2018.